Catalpol ameliorates doxorubicin-induced inflammation and oxidative stress in H9C2 cells through PPAR-γ activation

YANJIE JIANG[1] and QING ZHANG[2]

[1]Department of Pharmacology, Jinhua Institute for Food and Drug Control, Jinhua, Zhejiang 321017;
[2]Department of Pharmacy, Lianshui County People's Hospital, Huai'an, Jiangsu 223400, P.R. China

Abstract. Drug-induced cardiomyopathy is a severe disease that leads to refractory heart disease at late stages, with increasing detrimental effects. DOX-induced cell damage is primarily induced via cellular oxidative stress. The present study investigated the effects of catalpol on doxorubicin (DOX)-induced H9C2 cardiomyocyte inflammation and oxidative stress. The Cell Counting Kit-8 assay was performed to detect cell viability, and western blotting was performed to detect the expression of peroxisome proliferator-activated receptor (PPAR)-γ in H9C2 cells. The expression levels of tumor necrosis factor-α (TNF-α), interleukin (IL)-1β and IL-6 were measured using ELISAs. Furthermore, the oxidative stress kit was used to detect the levels of malondialdehyde, superoxide dismutase and glutathione peroxidase. A reactive oxygen species (ROS) kit and DCF-DA staining were used to detect ROS levels. The results indicated that DOX treatment inhibited H9C2 cell expression of PPAR-γ and decreased H9C2 cell viability. Various concentrations of catalpol exhibited a less potent effect on H9C2 cell viability compared with DOX; however, catalpol increased the viability of DOX-induced H9C2 cells. Catalpol treatment also significantly decreased the expression levels of inflammatory factors (TNF-α, IL-1β and IL-6) in DOX-induced H9C2 cells, which was reversed by transfections with short hairpin RNA targeting PPAR-γ. Results from the present study indicated that catalpol ameliorated DOX-induced inflammation and oxidative stress in H9C2 cardiomyoblasts by activating PPAR-γ.

Introduction

Doxorubicin (DOX) is a highly effective and widely used chemotherapeutic agent for the treatment of human tumors, including solid tumors and hematological malignancies (1,2). However, the severe cardiotoxic side effects associated with DOX have limited its application in the clinic (1). DOX-induced cardiomyopathy may be caused by a variety of factors, including oxidative stress (3); however, the exact mechanisms underlying DOX-induced cardiomyopathy are not completely understood. Cancer chemotherapy-associated heart disease is a main cause of the increased mortality of cancer survivors (4,5); therefore, investigating the mechanisms of action of anthracyclines, including DOX, is important for the treatment of tumors and cardiovascular diseases.

As the main active ingredient in *Rehmannia*, catalpol belongs to the class of iridoid monosaccharides (6). Previous studies have demonstrated that catalpol exhibits a variety of biological activities, including anti-inflammatory (7-9), antioxidant (10,11), antiapoptotic (12,13) and hypoglycemic (14,15) effects. Previous studies investigating catalpol have primarily focused on its protective effects in the nervous system, and research into the effects of the compound on the cardiovascular system is in the early stages (16-18). Previous studies have reported that catalpol displays protective effects on cardiomyocytes at the cellular level, protecting against myocardial injury through antioxidation and ameliorating cardiac dysfunction in rat models (19,20). However, further studies are required to verify the cardiovascular protective effects of catalpol.

Peroxisome proliferator-activated receptor (PPAR) is a ligand-inducible transcription factor that is a member of the type II nuclear receptor superfamily. PPAR is primarily expressed in vascular smooth muscle cells, where it activates receptors, prevents proliferation and migration of vascular smooth muscle cells, weakens vascular remodeling, exerts anti-inflammatory and antiproliferative effects, and protects against pulmonary hypertension (21,22). It has also been reported that PPAR-γ receptors are also involved in the development of a variety of cardiovascular diseases. Moreover, PPAR-γ displays a range of physiological effects, including anti-inflammatory and antiatherosclerotic activities, and improving left ventricular remodeling (23,24). PPAR-γ also displays a protective effect against kidney and brain tissue ischemia-reperfusion injury (25,26); however, whether PPAR-γ displays a protective effect against myocardial ischemia-reperfusion injury has not been previously reported.

Correspondence to: Mr. Qing Zhang, Department of Pharmacy, Lianshui County People's Hospital, 6 Hongri Road, Huai'an, Jiangsu 223400, P.R. China
E-mail: bmzhangq@163.com

The present study aimed to investigate the protective effects of catalpol against DOX-induced inflammation and oxidative stress in H9C2 cardiomyoblasts, and to explore the possible mechanisms associated with PPAR-γ. The results of the present study may provide a theoretical basis for the treatment of DOX-induced inflammation and oxidative stress in H9C2 cardiomyoblasts.

Materials and methods

Cell lines and reagents. H9C2 cells were obtained from The Cell Bank of Type Culture Collection of the Chinese Academy of Sciences. Cells were cultured in DMEM (Gibco; Thermo Fisher Scientific, Inc.) supplemented with 10% inactivated fetal bovine serum (Gibco; Thermo Fisher Scientific, Inc.), 2 ml glutamine, 100 U/ml penicillin and streptomycin at 37°C with 5% CO_2. Catalpol (purity >98.0%) and DOX were purchased from the National Institute for the Control of Pharmaceutical and Biological Products. H9C2 cells were cultured with various concentrations of DOX (0, 0.1, 1 and 10 μM) for 12 and 24 h at 37°C. The same cells were also treated with various concentrations of catalpol (0, 10, 20, 40 and 80 μM) for 24 h at 37°C.

Cell Counting Kit-8 (CCK-8) assay. H9C2 cells were seeded (0.5×10^3 cells/ml) into 96-well plates and incubated with various concentrations of DOX (0, 0.1, 1 and 10 μM) for 12 and 24 h at 37°C (0 μM as control group). Subsequently, 10 μl CCK-8 reagent (Roche Diagnostics) was added to each well according to the manufacturer's protocol and incubated for 2 h at 37°C. The optical density of each well was measured at a wavelength of 490 nm using a microplate reader.

To confirm the effect of catalpol on H9C2 cells, H9C2 cells were cultured with various concentrations of catalpol (0, 10, 20, 40 and 80 μmol/l) for 24 h at 37°C (0 μM as control group). Then, to confirm the effect of DOX-induced H9C2 cardiomyocytes, catalpol administration in each dose group (10, 20, 40 and 80 μmol/l) after H9C2 cells treatment with DOX (1 μM) for 24 h at 37°C, respectively. According to the aforementioned method, 10 μl CCK-8 regent was added to each well in accordance with the manufacturer's protocol and incubated for 2 h at 37°C. The optical density of each well was measured at a wavelength of 490 nm using a microplate reader.

Transfection. The lentiviral vectors encoding PPAR-γ shRNA or control shRNA lentiviral particles were generated via 293T cell co-transfection with the PPAR-γ-shRNA plasmid vector (sc-156077-V) or the control shRNA Lentiviral Particles (sc-108080; each, Santa Cruz Biotechnology, Inc.). Short hairpin (sh)RNAs targeting PPAR-γ (shRNA-PPAR-γ-1 and shRNA-PPAR-γ-2) and an appropriate negative control (NC; non-targeting shRNA) were transfected into H9C2 cells (all, 4 μm). Then, the cells H9C2 transfected with shRNA-PPAR-γ subsequently treated either Dox/catalpol. shRNAs were designed and synthesized by Guangzhou RiboBio Co., Ltd. H9C2 cells were seeded into 6-well plates and at 70-80% confluence, transfection was performed using Opti-MEM Medium, serum-free DMEM and Lipofectamine® 2000 (Invitrogen; Thermo Fisher Scientific, Inc.), according to the manufacturer's protocol. Subsequently, cells were cultured for 24-72 h at 37°C. Transfection efficiency was determined by western blotting and RT-qPCR.

Western blotting. H9C2 cells were harvested and total protein was extracted using RIPA lysis buffer (Beyotime Institute of Biotechnology). Total protein was quantified using the bicinchoninic acid method. Proteins (30 μg/lane) were separated by 10% SDS-PAGE and transferred to PVDF membranes (EMD Millipore). After blocking with 5% milk for 2 h at room temperature, the membranes were incubated overnight at 4°C with primary antibodies against: PPAR-γ (cat. no. sc-7273; 1:1,000; Santa Cruz Biotechnology, Inc.) and GAPDH (cat. no. ab181602; 1:2,000; Abcam). Following primary incubation, the membranes were incubated with a goat anti-mouse IgG horseradish peroxidase-conjugated secondary antibody (cat. no. sc-2005; 1:10,000; Santa Cruz Biotechnology, Inc.) and a horseradish peroxidase-conjugated goat anti-rabbit IgG H&L antibody (cat. no. ab205718; 1:10,000; Abcam) at room temperature for 2 h. Protein bands were visualized using an ECL detection reagent (EMD Millipore). Blots were performed in triplicate and protein expression was quantified using ImageJ software (version 1.43; National Institutes of Health) with GAPDH as the loading control and for normalization.

Reverse transcription-quantitative PCR (RT-qPCR). H9C2 cell total RNA was extracted using the TRIzol reagent (Invitrogen; Thermo Fisher Scientific, Inc.) and stored at -40°C. Total RNA samples were thawed on ice and was reverse transcribed into cDNA using the PrimeScript RT reagent (Takara Bio, Inc.), according to the manufacturer's protocol. Subsequently, qPCR was performed using SYBR Green Master Mix I (Takara Bio, Inc.) and the ABI 7900 Fast Real-Time PCR system (Applied Biosystems; Thermo Fisher Scientific, Inc.). The following primers were used for qPCR: PPAR-γ, forward 5'-CAAGAC AACCTGCTACAAGC-3', reverse 5'-TCCTTGTAGATCTCC TGCAG-3'; GAPDH, forward 5'-CCAGGGGTGCCTTCT CTT-3', reverse 5'-CCGTGGGTAGAGTCATACTGG-3'. The following thermocycling conditions were used for qPCR: Initial denaturation at 95°C for 5 min; followed by 45 cycles of amplification, including denaturation at 95°C for 30 sec, annealing at 60°C for 30 sec and a final extension at 72°C for 10 min. mRNA expression levels were quantified using the $2^{-\Delta\Delta Cq}$ method and normalized to the internal reference gene GAPDH (27).

ELISA. Detection of reactive oxygen species (ROS), malondialdehyde (MDA), superoxide dismutase (SOD) and glutathione peroxidase (GSH-Px) levels in the H9C2 cell culture medium were measured by ELISA using commercial ELISA kits for Reactive Oxygen Species (ROS) Assay Kit 520 nm (cat. no. 88-5930; Thermo Fisher Scientific, Inc.), MDA ELISA kit (cat. no. AMS.E-EL-0060; Whuan Boster Biological Technology, Ltd.), SOD Human ELISA kit (cat. no. BMS222; Thermo Fisher Scientific, Inc.) and High Throughput Glutathione Peroxidase Assay kit (cat. no. 7512-100-K; R&D Systems, Inc.). The expression levels of tumor necrosis factor (TNF)-α (cat. no. ADI-901-099; NeoBioscience Technology Co., Ltd.), interleukin (IL)-1β (cat. no. EHC002b.48; NeoBioscience Technology Co., Ltd.)

and IL-6 (cat. no. ADI-901-033; NeoBioscience Technology Co., Ltd.) were detected using ELISA kits according to the manufacturer's protocol. The levels were quantified using Multiskan Mk3 microplate reader (Thermo Fisher Scientific, Inc.) to detect the concentration.

DCF-DA staining. H9C2 cells were seeded into 6-well plates, incubated for 24 h, washed twice with Earle's Balanced Salt Solution and subsequently incubated with 25 μM DCFH-DA for 30 min at 37˚C. Following the incubation, cells were washed twice with sugar Earle's solution. Fluorescence intensity was analyzed using a fluorescence reader (Fluoroscan Ascent FL; Thermo Labsystems) at an excitation wavelength of 488 nm and an emission wavelength of 525 nm. The images were obtained via confocal laser scanning microscopy (Olympus FV500; Olympus Corporation). Images were analyzed using ImageJ software (version 1.45; National Institutes of Health).

Statistical analysis. Data are expressed as the mean ± SD. All experiments were performed in triplicate. Statistical analyses were performed using SPSS (version 11.5; SPSS, Inc.) and GraphPad Prism (version 5; GraphPad Software, Inc.) software. Comparisons among groups were determined using one-way ANOVA followed by Tukey's or Dunnett's post hoc test. P<0.05 was considered to indicate a statistically significant difference.

Results

DOX inhibits the expression of PPAR-γ. Following treatment with various concentrations of DOX (0, 0.1, 1 and 10 μM) for 12 and 24 h, the protein expression levels of PPAR-γ in H9C2 cells were detected by western blotting. PPAR-γ expression levels decreased with increasing DOX concentrations (Fig. 1A). The results indicated that DOX inhibited the expression of PPAR-γ in a dose-dependent manner.

DOX affects H9C2 cell viability. Results from the CCK-8 assay indicated that the concentration of DOX (0.1 μM) had no significant effect on the viability of H9C2 cells, and that various concentrations of DOX (1 and 10 μM) significantly decreased H9C2 cell viability compared with the control group (P<0.05; Fig. 1B). As the IC_{50} of DOX at 24 h was ~1 μM, this concentration and duration were used for subsequent experiments.

Effect of catalpol on H9C2 cell viability. The results of the CCK-8 assay also indicated that H9C2 cell viability was not significantly altered following treatment with various concentrations of catalpol (0, 10, and 20 μM) for 24 h, but 40 and 80 μM catalpol significantly decreased H9C2 cell viability compared with the untreated control group (Fig. 2A).

Effect of catalpol on DOX-induced reductions to H9C2 cell viability. DOX treatment reduced viability, but co-treatment with catalpol reduced these effects. Additionally, H9C2 cell viability was significantly increased in the 10 μM catalpol+1 μM DOX group, the 20 μM catalpol+1 μM DOX group and the 40 μM catalpol+1 μM DOX group when compared with the 0 μM catalpol+1 μM DOX group (P<0.05;
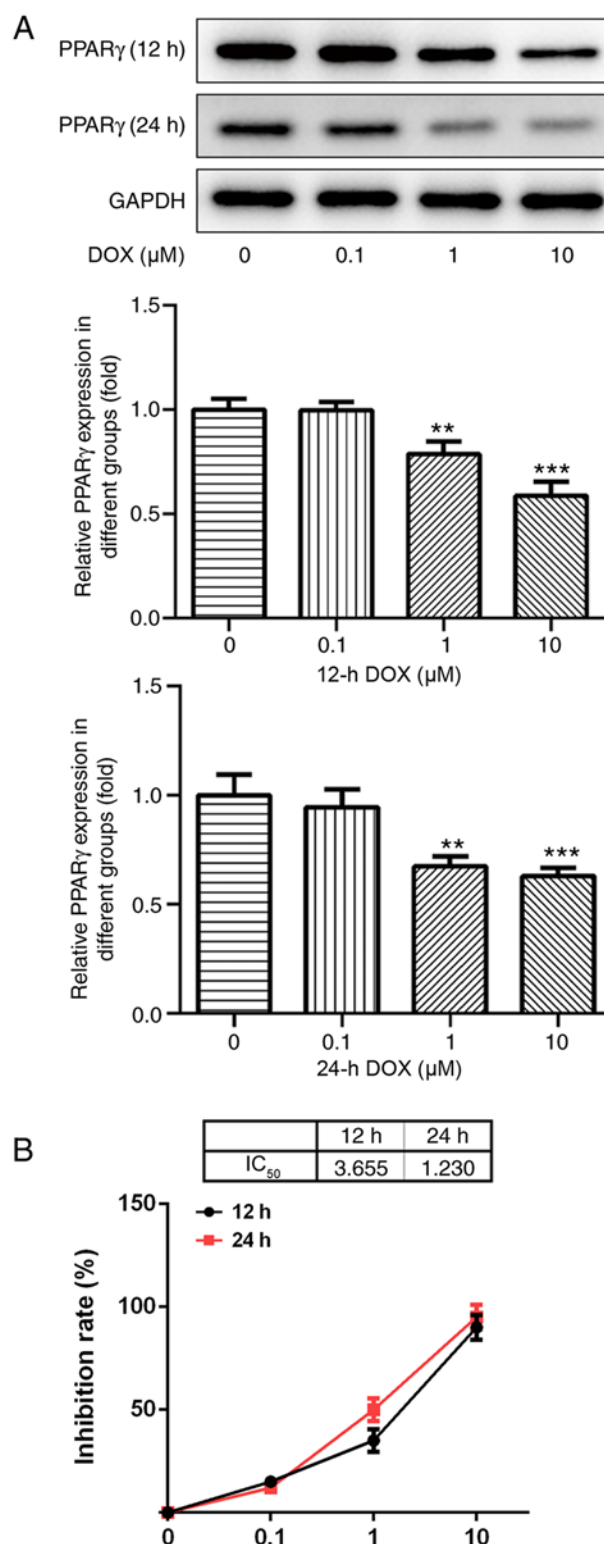

Figure 1. Effects of DOX on H9C2 PPAR-γ expression and cell viability. (A) PPAR-γ protein expression levels in H9C2 cells treated with various concentrations of DOX for 12 or 24 h were determined by western blotting. GAPDH was used as a loading control and for normalization of semi-quantified expression levels. (B) The Cell Counting Kit-8 assay was performed to assess the effects of DOX treatment on H9C2 cell viability. **P<0.01 and ***P<0.001 vs. 0 μM. DOX, doxorubicin; IC_{50}, half maximal inhibitory concentration; PPAR-γ, peroxisome proliferator-activated receptor-γ.

Fig. 2B). The results indicated that catalpol (10, 20 and 40 μM) attenuated DOX-induced effects on H9C2 cell viability and
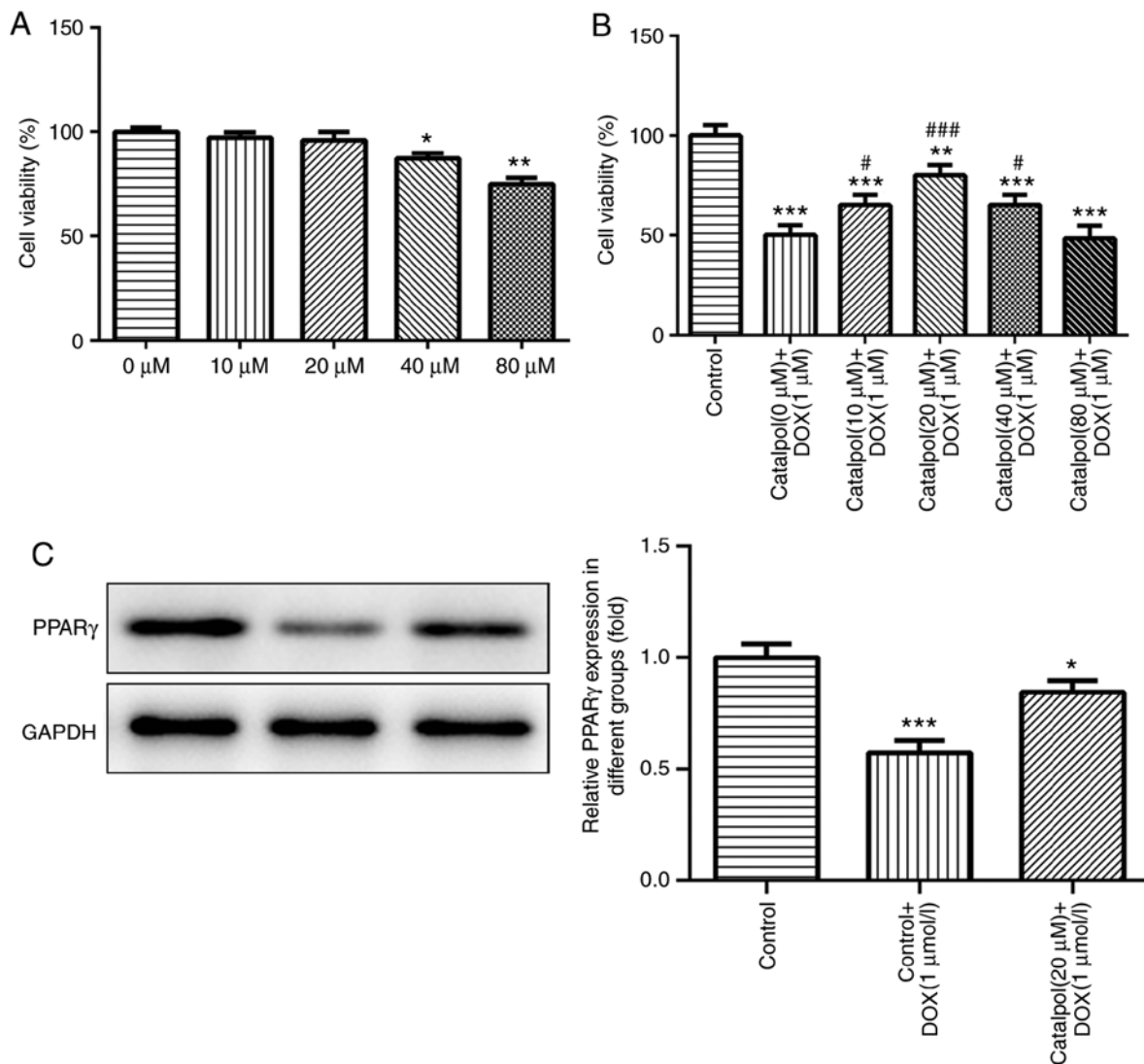
Figure 2. Effects of catalpol on DOX-induced effects in H9C2 cells. The Cell Counting Kit-8 assay was performed to assess H9C2 cell viability following treatment with various concentrations of (A) catalpol alone and (B) catalpol co-treatment with 1 μM DOX. (C) PPAR-γ protein expression levels were determined by western blotting. *P<0.05, **P<0.01 and ***P<0.001 vs. 0 μM or control; #P<0.01 and ###P<0.001 vs. Catalpol (0 μM) + DOX (1 μM). DOX, doxorubicin; PPAR-γ, peroxisome proliferator-activated receptor-γ.

80 μM catalpol significantly decreased H9C2 cell viability. Furthermore, 20 μM catalpol increased H9C2 cell viability to the highest level compared with other catalpol concentrations. Therefore, 20 μM catalpol was used for subsequent experimentation.

Catalpol serves a role in reducing DOX-induced cell damage via PPAR-γ. The expression of PPAR-γ was detected by western blotting. PPAR-γ expression levels in the DOX group were significantly lower compared with the control group; however, catalpol co-treatment increased PPAR-γ expression levels in the DOX group (Fig. 2C). The results indicated that catalpol serves a role in reducing DOX-induced cell damage via PPAR-γ.

Catalpol reduces DOX-induced inflammation and oxidative stress in H9C2 cells. The transfection efficiency of shRNA-PPAR-γ was detected by western blotting and RT-qPCR (Fig. 3A and B, respectively). The results suggested

that shRNA-PPAR-γ-1 and shRNA-PPAR-γ-2 significantly decreased PPAR-γ expression levels compared with the control group; however, the inhibitory effects of shRNA-PPAR-γ-1 were superior compared with shRNA-PPAR-γ-2 in H9C2 cells and was used in subsequent experiments.

The results of ELISA revealed that concentrations of the inflammatory factors TNF-α, IL-1β and IL-6 in the DOX group was significantly higher compared with the control group, and catalpol treatment significantly downregulated DOX-induced inflammatory factor expression (Fig. 4A). Furthermore, the expression of TNF-α, IL-1β and IL-6 in the 20 μM catalpol+1 μM DOX+ shRNA-PPAR-γ group was significantly upregulated compared with the 20 μM catalpol+1 μM DOX+ shRNA-NC group (Fig. 4A). Subsequently, the levels of oxidative stress-associated factors were examined. The levels of ROS and MDA were significantly increased in the DOX group compared with the control group, and catalpol co-treatment significantly downregulated DOX-induced ROS and MDA expression. The levels of ROS and MDA in the 20 μM
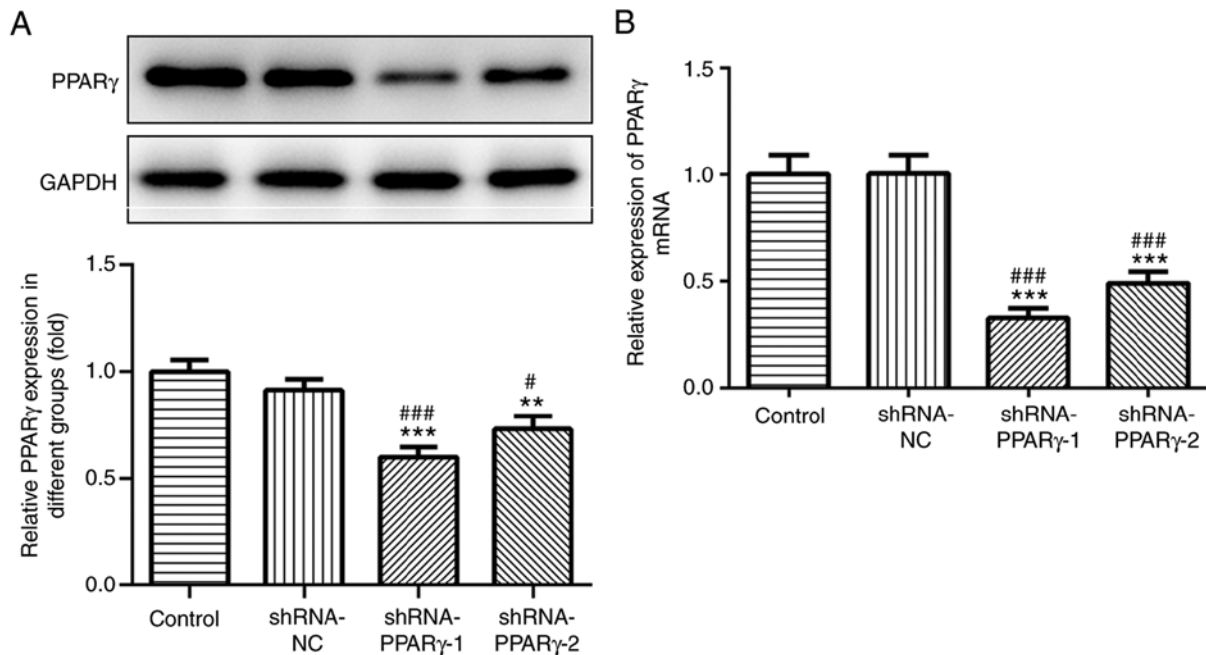
Figure 3. Transfection efficiency of shRNA-PPAR-γ-1 and shRNA-PPAR-γ-2. PPAR-γ (A) protein and (B) mRNA expression levels were determined by western blotting and reverse transcription-quantitative PCR, respectively. **P<0.01 and ***P<0.001 vs. control; #P<0.01 and ###P<0.001 vs. shRNA-NC. NC, negative control; PPAR-γ, peroxisome proliferator-activated receptor-γ; shRNA, short hairpin RNA.

catalpol+1 μM DOX+ shRNA-PPAR-γ group were significantly upregulated compared with the 20 μM catalpol+1 μM DOX+shRNA-NC group. SOD and GSH-Px displayed the opposite trend to ROS and MDA (Fig. 4B).

To further investigate ROS expression levels, DCF-DA staining was performed to detect the expression of ROS in H9C2 cells (Fig. 5). The fluorescence intensity in normal cardiomyocytes was generally weak with low ROS content. Following treatment with DOX for 24 h, the fluorescence intensity of the myocardial cells was enhanced and the fluorescence value was notably increased compared with the control group, indicating that the intracellular ROS content had increased. Compared with the DOX group, catalpol treatment significantly reduced the intracellular fluorescence intensity, the fluorescence value and the ROS content of H9C2 cells. However, the addition of shRNA-PPAR-γ significantly reversed catalpol-mediated downregulation of intracellular ROS content. These results indicated that catalpol treatment significantly reduced DOX-induced ROS production. Collectively, the results suggested that catalpol reversed DOX-induced inflammation and oxidative stress in H9C2 cells through PPAR-γ activation.

Discussion

Drug-induced cardiomyopathy is a severe disease that occurs independent of other cardiovascular risk factors, but is a widespread side effect of a number of therapeutic agents, such as Daunorubicin, DOX and Paclitaxel (28-30). As it is difficult to identify symptoms and signs during the early stages of the disease, drug-induced cardiomyopathy often leads to refractory heart disease in the late stages, with increasing detrimental effects (31,32). DOX-induced cardiomyopathy is the most common type of drug-induced heart disease (33).

DOX-induced damage to the heart has significantly limited its therapeutic use in the clinic (34). The main mechanism of action of DOX is inhibition of DNA double-strand break, DNA replication and DNA transcription by topoisomerase 2 inhibition. DOX also directly embeds into the DNA, induces reactive oxygen species production and regulates the binding of histone DNA (35,36). Furthermore, DOX sequesters iron ions to produce free radicals, which in turn trigger the initiation of apoptotic factor expression and promotes cell death (37). Therefore, DOX induces cardiomyocyte damage when it destroys tumor cells (4). Early myocardial damage manifests as myocarditis and arrhythmia; however, when DOX reaches a specific dose, irreversible myocardial expansion occurs, which may eventually develop into heart failure (38). Although numerous efforts have been made to reduce the toxicity of DOX, no significant progress in the prevention and treatment of DOX-induced toxicity has been reported. Therefore, the development of novel therapeutic agents and strategies for the prevention of DOX-induced myocardial damage is important.

Rehmannia glutinosa is one of the most commonly used Traditional Chinese Medicine, and it has been reported to lower blood sugar, regulate immunity, enhance hematopoietic functions and inhibit tumors. *R. glutinosa* also displays antiaging properties by exerting protective effects on the cardiovascular and vascular systems. Catalpol, an iridoid glycoside isolated from the roots of *R. glutinosa*, has been reported to display neuroprotective effects (38,39). Previous studies have also demonstrated the cardioprotective and anti-inflammatory properties of catalpol, including apoptosis inhibition, reduced neuronal death and promotion of differentiation (40,41). In a mouse model of lipopolysaccharide-induced acute lung injury, catalpol prevents injury by inhibiting TNF-α, IL-1β and IL-6 expression (42). However, the mechanisms underlying
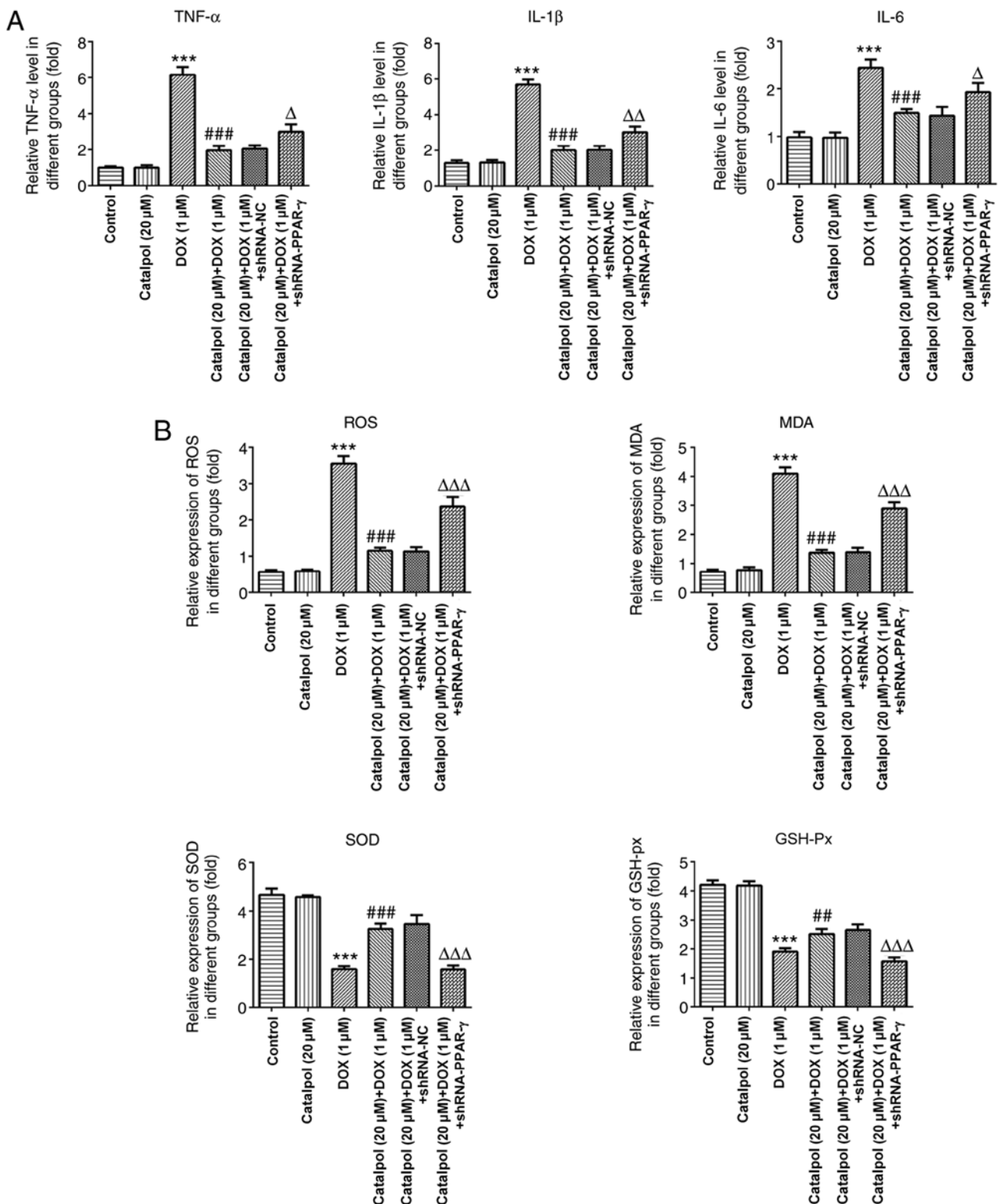
Figure 4. Catalpol relieves DOX-induced inflammation and oxidative stress in H9C2 cells. (A) Catalpol downregulates DOX-induced expression of the inflammatory factors TNF-α, IL-6 and IL-1β. (B) Catalpol downregulates DOX-induced expression of the oxidative stress factors ROS, MDA, SOD and GSH-Px in H9C2 cells. [**]P<0.001 vs. control; [##]P<0.05 and [###]P<0.001 vs. 1 μM DOX; [Δ]P<0.01, [ΔΔ]P<0.05 and [ΔΔΔ]P<0.001 vs. shRNA-NC. DOX, doxorubicin; GSH-Px, glutathione peroxidase; IL, interleukin; MDA, malondialdehyde; NC, negative control; PPAR-γ, peroxisome proliferator-activated receptor-γ; ROS, reactive oxygen species; shRNA, short hairpin RNA; SOD, superoxide dismutase; TNF-α, tumor necrosis factor-α.

the effects of catalpol on inflammation are not completely understood.

DOX has a potent toxic effect on cardiomyocytes and can alter cell morphology, induce cell death and promote apoptosis

through a series of molecular mechanisms (2,43,44). Therefore, identifying whether catalpol can attenuate the effects of DOX on myocardial cell survival is important. In the present study, H9C2 cell viability was significantly reduced in the DOX
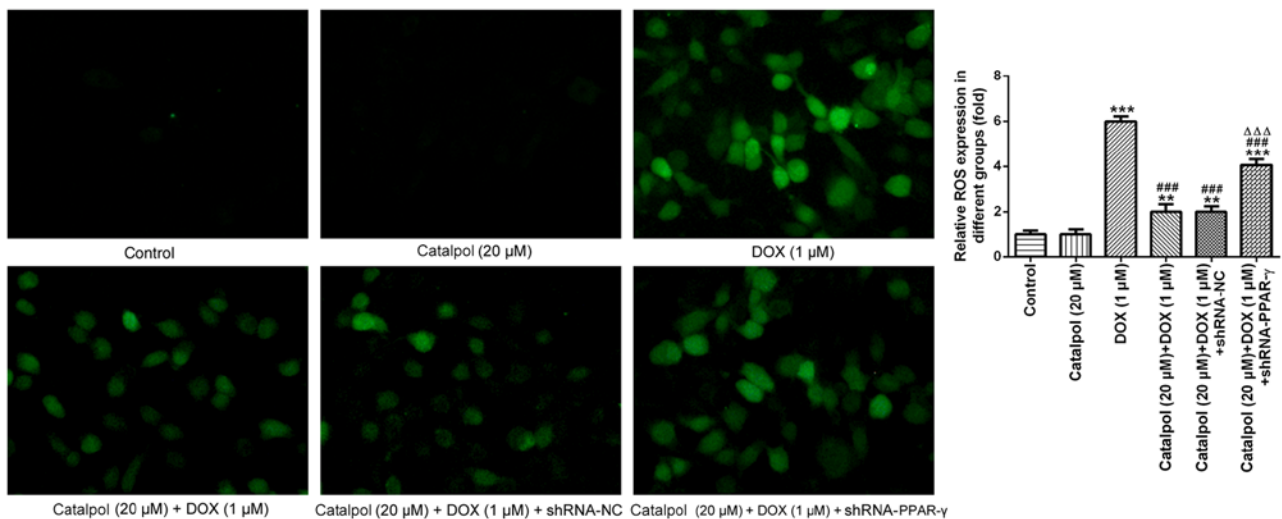
Figure 5. ROS levels of H9C2 cells determined by DCF-DA staining. shRNA- PPAR-γ-1 was transfected into H9C2 cells treated with Catalpol (0 μM) and DOX (1 μM), and incubated for 24 h. Subsequently, ROS levels were detected by DCF-DA staining (magnification, x400). [**]P<0.01 and [***]P<0.001 vs. control; [###]P<0.001 vs. DOX (1 μM); [ΔΔΔ]P<0.001 vs. catalpol (20 μM) + DOX (1 μM) + shRNA-NC. ROS, reactive oxygen species; shRNA, short hairpin RNA; DOX, doxorubicin; NC, negative control; PPAR-γ, peroxisome proliferator-activated receptor-γ.

group compared with the control group, which indicated that DOX displayed an inhibitory effect on cardiomyocyte survival. Furthermore, compared with the DOX group, H9C2 cells treated with catalpol displayed significantly increased cell viability, suggesting that catalpol attenuated the inhibitory effects of DOX on myocardial cell survival. The results indicated that the 20 μM catalpol group displayed the optimal protective effect, which suggested that catalpol reduced DOX-induced cardiomyocyte damage.

A previous study has reported that catalpol displays potent antioxidant effects, and DOX-induced cell damage is primarily induced via cellular oxidative stress (45). The initiation of oxidative stress in cardiomyocytes increases intracellular oxygen free radical production, and damages cells by attacking cell membranes and the mitochondria (46). Catalpol can reduce the generation of oxygen free radicals to decrease cell damage (47). The present study demonstrated that DOX increased the toxicity of cardiomyocytes, and reduced the ability of cells to resist oxidation. Our results indicating that catalpol reduced cardiomyocyte toxicity compared with the DOX group.

The inflammatory response is a defensive response of the body to damaging factors, involving several types of cells and cytokines, such as white blood cells, neutrophils, TNF-α, IL-1β and IL-6 (48,49). An increase in inflammatory cytokine levels is a sign of an inflammatory reaction in the body, which can induce the adhesion and migration of neutrophils and vascular endothelial cells, as well as the accumulation of neutrophils in myocardial tissue, the release of lysosomal enzymes and myocardial cell damage (50). TNF-α induces inflammation by activating inflammatory cells, including neutrophils, which mediate damage. TNF-α also displays direct cytotoxic effects, leading to alterations in the myocardial calcium balance and excitation-contraction coupling, as well as inducing apoptosis (51). A previous study has demonstrated that the mechanism underlying DOX-induced myocardial injury is complex (52). DOX damages myocardial tissue by

increasing the expression of inflammatory factors, including TNF-α, IL-1β and IL-6 (53). Similarly, TNF-α, IL-1β, IL-6 and other inflammatory factors are involved in the process of isoproterenol-induced myocardial injury (54). In the present study, the expression of TNF-α, IL-1β and IL-6 in the DOX group was significantly increased compared with the control group, which was consistent with the results of previous studies. The expression of inflammatory factors in the catalpol co-treatment group was significantly decreased, indicating that catalpol effectively prevented the DOX-induced inflammatory reaction in cardiomyocytes by inhibiting the release of inflammatory factors, thereby exerting a protective effect against myocardial injury.

To identify the possible mechanism underlying the anti-inflammatory activity of catalpol in cardiomyocytes, the present study focused on the role of PPAR-γ, as it has been reported that PPAR-γ receptors are also involved in the development of a variety of cardiovascular diseases, including inflammation, atherosclerosis and left ventricular remodeling (55-57). The present study demonstrated that catalpol acted to significantly increase PPAR-γ expression. Furthermore, to verify the effect of catalpol on PPAR-γ expression, H9C2 cells were treated with shRNA-PPAR-γ and 20 μM catalpol. The results suggested that PPAR-γ protein expression was inhibited at the transcriptional level after the addition of shRNA-PPAR-γ, and catalpol downregulated DOX-induced proinflammatory cytokine production. Collectively, the results indicated that catalpol played a role in DOX-induced cell damage by regulating PPAR-γ expression.

In conclusion, results from the present study indicated that DOX inhibited the expression of PPAR-γ and decreased H9C2 cardiomyocyte cell viability. Catalpol alleviated DOX-induced damage to H9C2 cardiomyocytes, potentially by reducing oxidative stress in cardiomyocytes. Therefore, the present study suggested that catalpol reversed DOX-induced H9C2 cardiomyocyte inflammation and oxidative stress by increasing PPAR-γ expression.

Authors' contributions

YJ designed the study, collected and analyzed the data, and drafted the manuscript. QZ conceived the study, contributed to the study design and critically revised the manuscript for important intellectual content. All authors read and approved the final manuscript.

Ethics approval and consent to participate

Not applicable.

Patient consent for publication

Not applicable.

Competing interests

The authors declare that they have no competing interests.

References

1. Rochette L, Guenancia C, Gudjoncik A, Hachet O, Zeller M, Cottin Y and Vergely C: Anthracyclines/trastuzumab: New aspects of cardiotoxicity and molecular mechanisms. Trends Pharmacol Sci 36: 326-348, 2015.
2. Smith LA, Cornelius VR, Plummer CJ, Levitt G, Verrill M, Canney P and Jones A: Cardiotoxicity of anthracycline agents for the treatment of cancer: Systematic review and meta-analysis of randomised controlled trials. BMC Cancer 10: 337, 2010.
3. Zhang YW, Shi J, Li YJ and Wei L: Cardiomyocyte death in doxorubicin-induced cardiotoxicity. Arch Immunol Ther Exp (Warsz) 57: 435-445, 2009.
4. Cardinale D, Colombo A, Bacchiani G, Tedeschi I, Meroni CA, Veglia F, Civelli M, Lamantia G, Colombo N, Curigliano G, et al: Early detection of anthracycline cardiotoxicity and improvement with heart failure therapy. Circulation 131: 1981-1988, 2015.
5. Gallucci G and Simeon V: Letter by Gallucci and Simeon regarding article, 'early detection of anthracycline cardiotoxicity and improvement with heart failure therapy'. Circulation 133: e362, 2016.
6. Chen Y, Liu Q, Shan Z, Zhao Y, Li M, Wang B, Zheng X and Feng W: The protective effect and mechanism of catalpol on high glucose-induced podocyte injury. BMC Complement Altern Med 19: 244, 2019.
7. Zhang X, Jin C, Li Y, Guan S, Han F and Zhang S: Catalpol improves cholinergic function and reduces inflammatory cytokines in the senescent mice induced by D-galactose. Food Chem Toxicol 58: 50-55, 2013.
8. Fu Q, Zhou Z, Li X, Guo H, Fan X, Chen J, Zhuang J, Zheng S and Zhu P: Protective effect of adenosine preconditioning against spinal cord ischemia-reperfusion injury in rats. Nan Fang Yi Ke Da Xue Xue Bao 34: 92-95, 2014 (In Chinese).
9. Bi J, Jiang B, Zorn A, Zhao RG, Liu P and An LJ: Catalpol inhibits LPS plus IFN-γ-induced inflammatory response in astrocytes primary cultures. Toxicol In Vitro 27: 543-550, 2013.
10. Zhang Z, Liu Y, Xue B and Wei L: Protective effects of catalpol against H$_2$O$_2$-induced oxidative damage in astrocytes. Zhongguo Zhong Yao Za Zhi 34: 1955-1958, 2009 (In Chinese).
11. Mao YR, Jiang L, Duan YL, An LJ and Jiang B: Efficacy of catalpol as protectant against oxidative stress and mitochondrial dysfunction on rotenone-induced toxicity in mice brain. Environ Toxicol Pharmacol 23: 314-318, 2007.
12. Hu L, Sun Y and Hu J: Catalpol inhibits apoptosis in hydrogen peroxide-induced endothelium by activating the PI3K/Akt signaling pathway and modulating expression of Bcl-2 and Bax. Eur J Pharmacol 628: 155-163, 2010.
13. Li DQ, Bao YM, Li Y, Wang CF, Liu Y and An LJ: Catalpol modulates the expressions of Bcl-2 and Bax and attenuates apoptosis in gerbils after ischemic injury. Brain Res 1115: 179-185, 2006.
14. Huang WJ, Niu HS, Lin MH, Cheng JT and Hsu FL: Antihyperglycemic effect of catalpol in streptozotocin-induced diabetic rats. J Nat Prod 73: 1170-1172, 2010.
15. Wang CF, Li DQ, Xue HY and Hu B: Oral supplementation of catalpol ameliorates diabetic encephalopathy in rats. Brain Res 1307: 158-165, 2010.
16. Yuan H, Ni X, Zheng M, Han X, Song Y and Yu M: Effect of catalpol on behavior and neurodevelopment in an ADHD rat model. Biomed Pharmacother 118: 109033, 2019.
17. Li Q, Yang T, Guo AC and Fan YP: Role of catalpol in ameliorating the pathogenesis of experimental autoimmune encephalomyelitis by increasing the level of noradrenaline in the locus coeruleus. Mol Med Rep 17: 4163-4172, 2018.
18. Zou G, Zhong W, Wu F, Wang X and Liu L: Inhibition of lncRNA Neat1 by catalpol via suppressing transcriptional activity of NF-κB attenuates cardiomyocyte apoptosis. Cell Cycle 18: 3432-3441, 2019.
19. Liu YR, Li PW, Suo JJ, Sun Y, Zhang BA, Lu H, Zhu HC and Zhang GB: Catalpol provides protective effects against cerebral ischaemia/reperfusion injury in gerbils. J Pharm Pharmacol 66: 1265-1270, 2014.
20. Cai Q, Yao Z and Li H: Catalpol promotes oligodendrocyte survival and oligodendrocyte progenitor differentiation via the Akt signaling pathway in rats with chronic cerebral hypoperfusion. Brain Res 1560: 27-35, 2014.
21. Youssef J and Badr M: Role of peroxisome proliferator-activated receptors in inflammation control. J Biomed Biotechnol 2004: 156-166, 2004.
22. Morgan MJ and Liu ZG: Crosstalk of reactive oxygen species and NF-κB signaling. Cell Res 21: 103-115, 2011.
23. Bishop-Bailey D: Peroxisome proliferator-activated receptors in the cardiovascular system. Br J Pharmacol 129: 823-834, 2000.
24. Geng DF, Wu W, Jin DM, Wang JF and Wu YM: Effect of peroxisome proliferator-activated receptor gamma ligand. Rosiglitazone on left ventricular remodeling in rats with myocardial infarction. Int J Cardiol 113: 86-91, 2006.
25. Singh AP, Singh N, Pathak D and Bedi PMS: Estradiol attenuates ischemia reperfusion-induced acute kidney injury through PPAR-γ stimulated eNOS activation in rats. Mol Cell Biochem 453: 1-9, 2019.
26. Otero-Losada M, LC, Udovin L, Kobiec T, Toro-Urrego N, A KR and Capani F: Long-term effects of hypoxia-reoxygenation on thioredoxins in rat central nervous system. Curr Pharm Des 25: 4791-4798, 2019.
27. Livak KJ and Schmittgen TD: Analysis of relative gene expression data using real-time quantitative PCR and the 2(-Delta Delta C(T)) method. Methods 25: 402-408, 2001.
28. Messinis DE, Melas IN, Hur J, Varshney N, Alexopoulos LG and Bai JPF: Translational systems pharmacology-based predictive assessment of drug-induced cardiomyopathy. CPT Pharmacometrics Syst Pharmacol 7: 166-174, 2018.
29. Yanagimoto K, Okamoto Y, Kodama Y, Nishikawa T, Tanabe T and Kawano Y: Decrease of cardiac base rotation in 2D speckle tracking indicates drug-induced cardiomyopathy after chemotherapy in children with cancer. J Pediatr Hematol Oncol 39: 10-14, 2017.
30. Helbock HJ, Beckman KB and Ames BN: 8-Hydroxydeoxyguanosine and 8-hydroxyguanine as biomarkers of oxidative DNA damage. Methods Enzymol 300: 156-166, 1999.
31. Rasheed S, Hashim R and Yan JS: Possible biomarkers for the early detection of HIV-associated heart diseases: A proteomics and bioinformatics prediction. Comput Struct Biotechnol J 13: 145-152, 2015.
32. Bizino MB, Jazet IM, Westenberg JJM, van Eyk HJ, Paiman EHM, Smit JWA and Lamb HJ: Effect of liraglutide on cardiac function in patients with type 2 diabetes mellitus: Randomized placebo-controlled trial. Cardiovasc Diabetol 18: 55, 2019

33. Xin YF, Wan LL, Peng JL and Guo C: Alleviation of the acute doxorubicin-induced cardiotoxicity by Lycium barbarum polysaccharides through the suppression of oxidative stress. Food Chem Toxicol 49: 259-264, 2011.

34. Hu J, Wu Q, Wang Z, Hong J, Chen R, Li B, Hu Z, Hu X and Zhang M: Inhibition of CACNA1H attenuates doxorubicin-induced acute cardiotoxicity by affecting endoplasmic reticulum stress. Biomed Pharmacother 120: 109475, 2019.

35. Riba A, Deres L, Eros K, Szabo A, Magyar K, Sumegi B, Toth K, Halmosi R and Szabados E: Doxycycline protects against ROS-induced mitochondrial fragmentation and ISO-induced heart failure. PLoS One 12: e0175195, 2017.

36. Chaudhari U, Nemade H, Gaspar JA, Hescheler J, Hengstler JG and Sachinidis A: MicroRNAs as early toxicity signatures of doxorubicin in human-induced pluripotent stem cell-derived cardiomyocytes. Arch Toxicol 90: 3087-3098, 2016.

37. Mjos KD, Cawthray JF, Jamieson G, Fox JA and Orvig C: Iron (III)-binding of the anticancer agents doxorubicin and vosaroxin. Dalton Trans 44: 2348-2358, 2015.

38. Medeiros-Lima DJM, Carvalho JJ, Tibirica E, Borges JP and Matsuura C: Time course of cardiomyopathy induced by doxorubicin in rats. Pharmacol Rep 71: 583-590, 2019.

39. Xu L, Zhang W, Zeng L and Jin JO: Rehmannia glutinosa polysaccharide induced an anti-cancer effect by activating natural killer cells. Int J Biol Macromol 105: 680-685, 2017.

40. Choi EM, Suh KS, Jung WW, Yun S, Park SY, Chin SO, Rhee SY and Chon S: Catalpol protects against 2,3,7,8-tetrachlorodibenzo-p-dioxin-induced cytotoxicity in osteoblastic MC3T3-E1 cells. J Appl Toxicol 39: 1710-1719, 2019.

41. Zou G, Zhong W, Wu F, Wang X and Liu L: Catalpol attenuates cardiomyocyte apoptosis in diabetic cardiomyopathy via Neat1/miR-140-5p/HDAC4 axis. Biochimie 165: 90-99, 2019.

42. Fu K, Piao T, Wang M, Zhang J, Jiang J, Wang X and Liu H: Protective effect of catalpol on lipopolysaccharide-induced acute lung injury in mice. Int Immunopharmacol 23: 400-406, 2014.

43. Štěrba M, Popelová O, Vávrová A, Jirkovský E, Kovaříková P, Geršl V and Šimůnek T: Oxidative stress, redox signaling, and metal chelation in anthracycline cardiotoxicity and pharmacological cardioprotection. Antioxid Redox Signal 18: 899-929, 2013.

44. Yu X, Cui L, Zhang Z, Zhao Q and Li S: α-Linolenic acid attenuates doxorubicin-induced cardiotoxicity in rats through suppression of oxidative stress and apoptosis. Acta Biochim Biophys Sin (Shanghai) 45: 817-826, 2013.

45. Zhao X, Jin Y, Li L, Xu L, Tang Z, Qi Y, Yin L and Peng J: MicroRNA-128-3p aggravates doxorubicin-induced liver injury by promoting oxidative stress via targeting Sirtuin-1. Pharmacol Res 146: 104276, 2019.

46. Wu S, Lu Q, Ding Y, Wu Y, Qiu Y, Wang P, Mao X, Huang K, Xie Z and Zou MH: Hyperglycemia-driven inhibition of AMP-activated protein kinase α2 induces diabetic cardiomyopathy by promoting mitochondria-associated endoplasmic reticulum membranes in vivo. Circulation 139: 1913-1936, 2019.

47. Li Y, Bao Y, Jiang B, Wang Z, Liu Y, Zhang C and An L: Catalpol protects primary cultured astrocytes from in vitro ischemia-induced damage. Int J Dev Neurosci 26: 309-317, 2008.

48. Chakraborty RK and Burns B: Systemic inflammatory response syndrome. In: StatPearls, Treasure Island (FL), 2020.

49. Ramadori P, Ahmad G and Ramadori G: Cellular and molecular mechanisms regulating the hepatic erythropoietin expression during acute-phase response: A role for IL-6. Lab Invest 90: 1306-1324, 2010.

50. Hu L, Mauro TM, Dang E, Man G, Zhang J, Lee D, Wang G, Feingold KR, Elias PM and Man MQ: Epidermal dysfunction leads to an age-associated increase in levels of serum inflammatory cytokines. J Invest Dermatol 137: 1277-1285, 2017.

51. Yamashita M and Passegue E: TNF-α coordinates hematopoietic stem cell survival and myeloid regeneration. Cell Stem Cell 25: 357-372 e357, 2019.

52. Faridvand Y, Haddadi P, Vahedian V, Nozari S, Nejabati HR, Pezeshkian M, Afrasiabi A, Safaie N, Jodati A and Nouri M: Human amnion membrane proteins prevent doxorubicin-induced oxidative stress injury and apoptosis in rat H9c2 cardiomyocytes. Cardiovasc Toxicol: Feb 21, 2020 doi: 10.1007/s12012-020-09564-8 (Epub ahead of print).

53. Han MS, White A, Perry RJ, Camporez JP, Hidalgo J, Shulman GI and Davis RJ: Regulation of adipose tissue inflammation by interleukin 6. Proc Natl Acad Sci USA 117: 2751-2760, 2020.

54. Cen W, Chen Z, Gu N and Hoppe R: Prevention of AMI induced ventricular remodeling: Inhibitory effects of heart-protecting musk pill on IL-6 and TNF-alpha. Evid Based Complement Alternat Med 2017: 3217395, 2017.

55. Terrasi M, Bazan V, Caruso S, Insalaco L, Amodeo V, Fanale D, Corsini LR, Contaldo C, Mercanti A, Fiorio E, et al: Effects of PPARγ agonists on the expression of leptin and vascular endothelial growth factor in breast cancer cells. J Cell Physiol 228: 1368-1374, 2013.

56. Tan NS, Michalik L, Desvergne B and Wahli W: Multiple expression control mechanisms of peroxisome proliferator-activated receptors and their target genes. J Steroid Biochem Mol Biol 93: 99-105, 2005.

57. Choo J, Lee Y, Yan XJ, Noh TH, Kim SJ, Son S, Pothoulakis C, Moon HR, Jung JH and Im E: A novel peroxisome proliferator-activated receptor (PPAR)γ agonist 2-hydroxyethyl 5-chloro-4,5-didehydrojasmonate exerts anti-inflammatory effects in colitis. J Biol Chem 290: 25609-25619, 2015.